Protective Effect of Intranasal Regimens Containing Peptidic Middle East Respiratory Syndrome Coronavirus Fusion Inhibitor Against MERS-CoV Infection

Rudragouda Channappanavar,[1,a] Lu Lu,[4,a] Shuai Xia,[4] Lanying Du,[5] David K. Meyerholz,[2] Stanley Perlman,[1,3] and Shibo Jiang[4,5]

[1]Departments of Microbiology, [2]Pathology, and [3]Pediatrics, University of Iowa, Iowa City; [4]Key Laboratory of Medical Molecular Virology of Ministries of Education and Health, Shanghai Medical College and Shanghai Public Health Clinical Center, Fudan University, China; and [5]Lindsley F. Kimball Research Institute, New York Blood Center, New York

To gain entry into the target cell, Middle East respiratory syndrome (MERS) coronavirus (MERS-CoV) uses its spike (S) protein S2 subunit to fuse with the plasma or endosomal membrane. Previous work identified a peptide derived from the heptad repeat (HR) 2 domain in S2 subunit, HR2P, which potently blocked MERS-CoV S protein–mediated membrane fusion. Here, we tested an HR2P analogue with improved pharmaceutical property, HR2P-M2, for its inhibitory activity against MERS-CoV infection in vitro and in vivo. HR2P-M2 was highly effective in inhibiting MERS-CoV S protein–mediated cell-cell fusion and infection by pseudoviruses expressing MERS-CoV S protein with or without mutation in the HR1 region. It interacted with the HR1 peptide to form stable α-helical complex and blocked six-helix bundle formation between the HR1 and HR2 domains in the viral S protein. Intranasally administered HR2P-M2 effectively protected adenovirus serotype-5–human dipeptidyl peptidase 4–transduced mice from infection by MERS-CoV strains with or without mutations in the HR1 region of S protein, with >1000-fold reduction of viral titers in lung, and the protection was enhanced by combining HR2P-M2 with interferon β. These results indicate that this combination regimen merits further development to prevent MERS in high-risk populations, including healthcare workers and patient family members, and to treat MERS-CoV–infected patients.

Keywords. MERS-CoV; fusion inhibitor; peptide; interferon.

Severe human respiratory infection caused by the Middle East Respiratory Syndrome (MERS) coronavirus (MERS-CoV) was first identified in 2012 [1]. As of 25 May 2015, a total of 1139 laboratory-confirmed cases and 431 deaths had been reported to the World Health Organization (http://www.who.int/csr/don/25-may-2015-mers-saudi-arabia/en/). The high case fatality rate among patients with MERS-CoV infection has caused widespread fear because the mode of transmission from zoonotic sources is not well understood, and coronaviruses have the potential to mutate, becoming more pathogenic and transmissible [1–4]. Bats and dromedary camels are considered to be the natural reservoir and intermediate hosts for MERS-CoV, respectively, but most community-acquired cases are not associated with camel contact [5–8]. Cumulative evidence from healthcare settings suggests that person-to-person transmission of MERS-CoV can occur through close contact [2, 9]. In the absence of an effective vaccine, it is essential to develop strategies to prevent camel-to-human and human-to-human transmission among high-risk populations, as well as to treat MERS-CoV–infected patients.

MERS-CoV, an enveloped, positive-sense, single-stranded RNA virus, binds to the target cell through

interaction between the receptor-binding domain in its spike (S) protein S1 subunit [10–14] and its receptor, dipeptidyl peptidase 4 (DPP4, also known as CD26) [15]. After binding and proteolytic cleavage, a fusion peptide at the N-terminus of S2 is exposed and is inserted into the plasma or endosomal membrane. The heptad repeat (HR) 2 binds to the HR1 in S2 to form a six-helix bundle (6-HB) fusion core, which brings viral and cell membranes into close apposition for fusion [16]. Peptides derived from the HR2 region, such as HR2P, can also interact with HR1 domain in the viral S protein to form heterogeneous 6-HB and thus block viral fusion with host cell membranes [16], as described elsewhere in the context of human immunodeficiency virus (HIV) and severe acute respiratory syndrome (SARS)–CoV infections [17–20].

In the present study, we evaluated an HR2P analogue, designated HR2P-M2, for its in vitro and in vivo efficacy against infection by the MERS-CoV Erasmus Medical Center (EMC)/2012 strain and strains with mutations in the HR1 domain of the S protein. Most notably, we determined the prophylactic and therapeutic protective activity of HR2P-M2 when used alone or in combination with interferon (IFN) β in human DPP4 receptor (hDPP4)–transduced mice challenged with MERS-CoV.

MATERIALS AND METHODS

Cells and Viruses
293T cells and Huh-7 cells were obtained from American Type Culture Collection and the Cell Bank of the Chinese Academy of Science, respectively. The EMC/2012 strain of MERS-CoV (passage 8, designated MERS-CoV), provided by Drs Bart Haagmans and Ron Fouchier (EMC), was passaged once on Vero 81 cells. Adenovirus serotype 5 (Ad5)-hDPP4 was developed and propagated by the University of Iowa Gene Transfer Vector Core.

Circular Dichroism Spectroscopic Analysis
Circular dichroism spectroscopy was used to determine the secondary structure of the peptides and their complexes [16, 21–23], as described elsewhere. After this analysis, thermal denaturation of peptide complexes was immediately monitored using the same sample from 4°C to 100°C at 222 nm with a thermal gradient of 5°C min^{-1}. The [θ]222 value of −33 000 degrees cm^2 dmol^{-1} was taken as 100% α-helical content [16, 17, 21]. Data were further processed using Jasco software.

Native Polyacrylamide Gel Electrophoresis
Native polyacrylamide gel electrophoresis (N-PAGE) was performed as described elsewhere [19, 22]. Peptide HR1P/ HR1P-Q1020R/HR1P-Q1020R (40 μmol/L in phosphate-buffered saline [PBS]) was incubated with peptide HR2P-M2 (40 μmol/L) at 37°C for 30 minutes, respectively, using PBS as control, followed by loading on an 18% Tris-glycine gel with tricine glycine running buffer (pH 8.3). After staining with

Coomassie blue, images were acquired on a FluorChem Imaging System (Alpha Innotech/ProteinSimple).

Fluorescence N-PAGE
Fluorescence N-PAGE (FN-PAGE) was carried out in the same manner described above for N-PAGE, except using fluorescein isothiocyanate–conjugated peptide (HR2P-F). Peptide HR1P, HR1P-Q1020H, or HR1P-Q1020R, respectively, at 40 μmol/L in PBS was incubated with peptide HR2P-F (40 μmol/L) at 37°C for 30 minutes to form 6-HB, or incubated with increasing concentrations (40, 60, and 80 μmol/L) of HR2P-M2 in PBS at 37°C for 30 minutes, before addition of HR2P-F followed by incubation with HR2P-F (40 μmol/L) at 37°C for another 30 minutes to inhibit 6-HB formation. Gels were imaged using a FluorChem 8800 Imaging system with excitation wavelength at 302 nm and emission wavelength at 520 nm. After imaging, the gel was stained with Coomassie blue and reimaged.

Inhibition of MERS-CoV S Protein–Mediated Cell-Cell Fusion
MERS-CoV S protein–mediated cell-cell fusion was tested as described elsewhere [16]. 293T cells transfected with plasmid pAAV-IRES-MERS-EGFP (293T/MERS/EGFP), pAAV-IRES-MERS-Q1020H/EGFP (293T/MERS-Q1020H/EGFP), or pAAV-IRES-MERS-Q1020R/EGFP (293T/MERS-Q1020R/ EGFP), respectively, coexpressing the MERS-CoV S protein and EGFP on cell surface, were used as effector cells whereas 293T/EGFP cells, expressing only EGFP were used as negative control cells. 293T/MERS/EGFP (or 293T/MERS-Q1020H/ EGFP, or 293T/MERS-Q1020R/EGFP) and 293T/EGFP cells (1×10^4) were incubated with Huh-7 cells expressing the MERS-CoV receptor DPP4 (5×10^4) as target cells, in the absence or presence of test peptides at the indicated concentrations for 2–4 hours at 37°C. 293T/MERS/EGFP and 293T/ EGFP cells fused, or unfused, with Huh-7 cells were counted under an inverted fluorescence microscope (Nikon Eclipse Ti-S) and the median inhibitory concentration (IC$_{50}$) was calculated using the CalcuSyn software [24].

Inhibition of Pseudotyped MERS-CoV Infection
Pseudoviruses carrying MERS-CoV S protein with or without mutations were produced as described elsewhere [25, 26]. Briefly, pseudovirus was incubated with a test peptide at graded concentrations at 37°C for 1 hour, followed by addition of the virus/peptide mixture to Huh-7 cells. Cultures were refed with fresh medium 12 hours after infection and incubated for another 48 hours at 37°C, followed by addition of luciferase substrate (Promega). Fluorescence was assessed using a luciferase kit (Promega) and an Ultra 384 luminometer (Tecan).

Mice
Specific pathogen-free 6–12-week-old C57BL/6 mice and RAG1$^{-/-}$ mice were purchased from the National Cancer Institute and the Jackson Laboratory, respectively, and bred at the

University of Iowa. All studies were carried out in strict accordance with the recommendations in the *Guide for the Care and Use of Laboratory Animals* from the National Institutes of Health. Animal experiments were approved by the Institutional Animal Care and Use Committee at the University of Iowa (protocol 4041009).

Transduction and Infection of Mice

C57BL/6 and RAG1$^{-/-}$ mice were transduced intranasally with 2.5×10^8 plaque-forming units (PFUs) of Ad5-hDPP4 in 75 μL of Dulbecco's modified Eagle medium (DMEM). Five days after transduction, mice were infected intranasally with wild-type (WT) or mutant MERS-CoV (10^5 PFUs/50 μL of DMEM) and treated intranasally with 50 μL of PBS or HR2P-M2 (200 μg) peptide, alone or in combination with IFN-β. All work with MERS-CoV was conducted in the University of Iowa's biosafety level 3 laboratory.

Viral Titers

Lung viral titers were determined using Vero 81 cells, as described elsewhere [27]. Viral titers are expressed as plaque-forming units per gram of lung tissue.

Construction of Recombinant Viruses

Recombinant bacterial artificial chromosomes (BACs) with Q1020R/H mutations were engineered using the Kan^R-I-SceI marker cassette for positive and negative selection, as described elsewhere [28]. pBAC-MERS-CoV (a generous gift from Luis Enjuanes) was transformed into GS1783 *Escherichia coli* cells (a generous gift from Greg Smith) containing an arabinose-inducible I-SceI restriction enzyme. A polymerase chain reaction product was generated and transformed into GS1783 cells and recombined with pBAC-MERS-CoV. Recombinant BACs were selected on Luria–Bertani-chloramphenicol-kanamycin plates and verified by restriction enzyme digestion and polymerase chain reaction. The resulting BAC clone was termed pBAC-MERS-CoV Q1020R/H.

RESULTS

Inhibition of HR2P-M2 on MERS-CoV S Protein–Mediated Cell-Cell Fusion and Infection by Pseudoviruses Carrying MERS-CoV S Protein With Mutations in HR1 Domain

We tested the inhibitory activity of peptide HR2P-M2, a variant of HR2P (Figure 1A), on MERS-CoV S protein–mediated cell-cell fusion, using as controls peptides MERS HR2P and SARS CP-1, derived from the HR2 domain of MERS-CoV and SARS-CoV S proteins, respectively [16, 19]. Both HR2P-M2 and HR2P strongly inhibited S protein–mediated cell-cell fusion in a dose-dependent manner, with IC$_{50}$ values of 0.55 and 0.97 μmol/L, respectively (Figure 1B), indicating that HR2P-M2 has improved membrane fusion inhibitory activity compared with HR2P. SARS CP-1 peptide did not inhibit MERS-CoV S–mediated cell-cell fusion at concentrations up

to 20 μmol/L, confirming a previous observation by Lu et al [16]. The MERS-CoV S protein HR1 domain, the target site of HR2-derived peptides (eg, HR2P and HR2P-M2), has largely conserved sequences when different strains are compared. Among clinical MERS-CoV strains, only 1 amino acid change at position 1020 of the HR1 domain (Q1020H or Q1020R) (Figure 1A) was observed, and this was present in nearly all strains [29, 30]. To test whether HR2P-M2 was effective against these MERS-CoV strains, we compared the inhibitory activity of HR2P-M2 on cell-cell fusion mediated by MERS-CoV S protein, with or without Q1020H or Q1020R mutations. Surprisingly, HR2P-M2 was about 0.9–2.6-fold more potent in inhibiting cell-cell fusion mediated by MERS-CoV S protein bearing Q1020H and Q1020R, respectively, than the WT S protein of the EMC/2012 strain (Figure 1C).

Subsequently, we compared HR2P-M2 with HR2P and SARS CP-1 for their inhibitory activity on the entry of pseudovirus expressing MERS-CoV S protein. As shown in Figure 1D, HR2P-M2 was also more potent than HR2P, with IC$_{50}$ values of 0.61 and 1.21 μmol/L, respectively, whereas, again, CP-1 exhibited no inhibition at concentrations up to 20 μmol/L. We then constructed pseudoviruses expressing MERS-CoV S protein with Q1020H or Q1020R mutations and compared their sensitivity with that of HR2P-M2. Similarly, HR2P-M2 was about 5–8-fold more effective at inhibiting infection by the pseudoviruses carrying mutant S protein (Q1020H or Q1020R) than infection by the pseudovirus carrying the WT S protein, whereas CP-1 displayed no inhibition of either mutant MERS-CoV pseudovirus (Figure 1E and 1F). These results suggest that HR2P-M2 is expected to be effective against all MERS-CoV strains isolated so far.

Interaction of HR2P-M2 With HR1 Peptide to Form a Stable α-Helical Complex and Block 6-HB Formation Between HR1 and HR2 Peptides

Lu et al [16] showed previously that peptides derived from the MERS-CoV S protein HR1 and HR2 domain (HR1P and HR2P, respectively) could interact together to form stable α-helical complex with α-helicity of approximately 76% and a thermal unfolding transition (Tm) value of 87°C. Using circular dichroism spectroscopy, we compared the secondary structures of HR2P-M2, HR1P and its mutants (HR1P-Q1020H and HR1P-Q1020R), and the complexes formed between HR1 and HR2 peptides. As shown in Figure 2A–C, HR2P-M2 showed low α-helicity (approximately 6%), whereas all the HR1 peptides displayed random structures. However, all the complexes formed between HR2P-M2 and the HR1 peptides exhibited α-helical structure with α-helicity in the range of 79%–88% (Figure 2A–C), in addition to high Tm values (91°C–95°C) (Figure 2D), suggesting that HR2P-M2 can interact with all these HR1 peptides to form highly stable α-helical complexes.

We then used N-PAGE and FN-PAGE [16, 19, 22] to further investigate the interaction between HR2P-M2 and HR1P or its
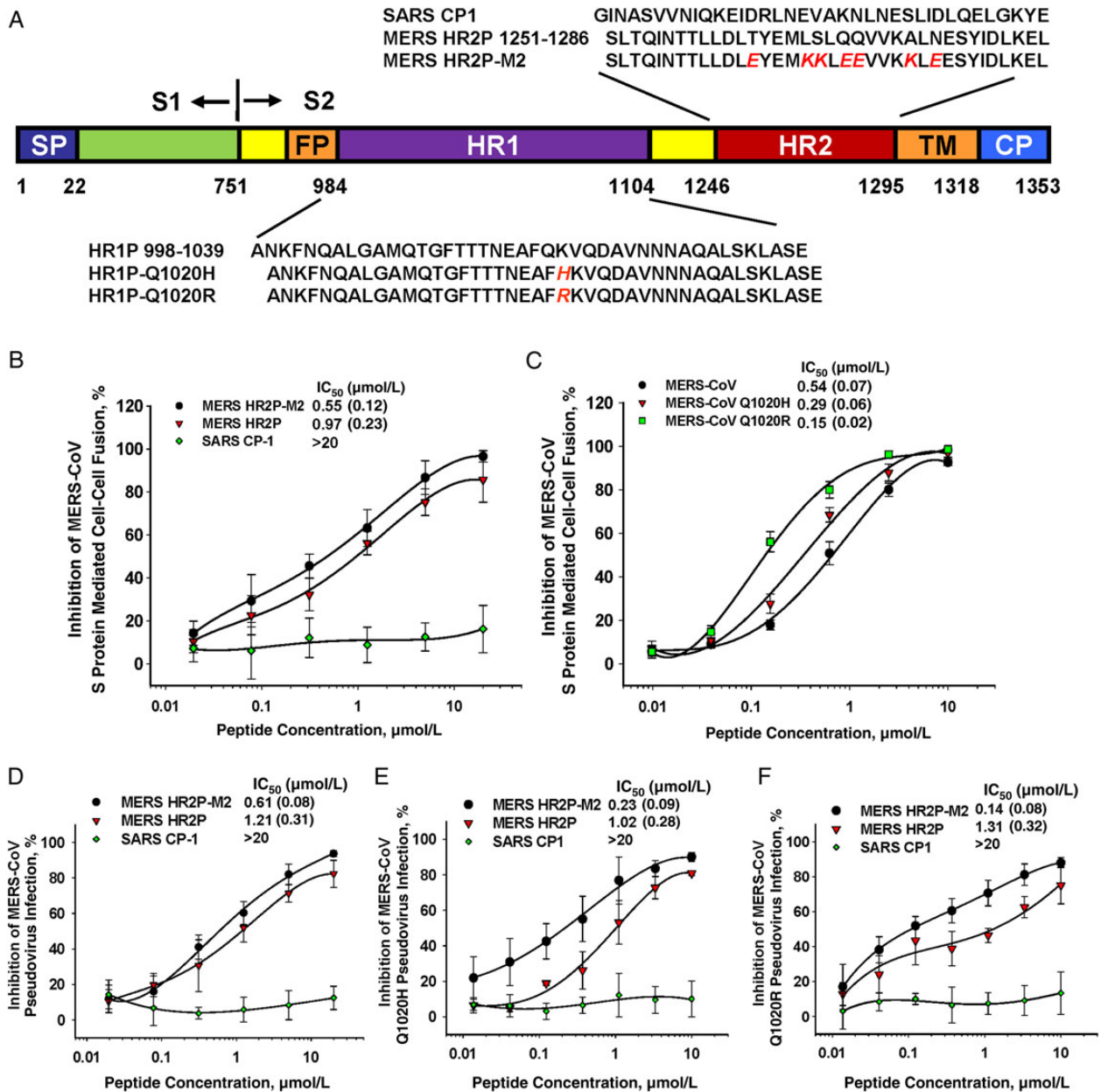
Figure 1. Schematic illustration of the Middle East respiratory syndrome coronavirus (MERS-CoV) S2 subunit HR1 and HR2 domains and inhibition of MERS-CoV infection. *A*, Sequences of peptides derived from HR1 and HR2 domains of the MERS-CoV spike (S) protein S2 subunit. *B, C*, Inhibition of cell-cell fusion mediated by MERS-CoV S protein without mutation (*B*) and with Q1020H or Q1020R mutation (*C*). *D–F*, Inhibition of infection by pseudoviruses expressing S protein of MERS-CoV EMC/2012 strain (*D*), or S protein with Q1020H (*E*) or Q1020R (*F*). Each sample was tested in triplicate, and the experiment was repeated twice. Data from a representative experiment are shown as means with standard deviation (*bars*). Abbreviations: CP, cytoplasmic domain; EMC, Erasmus Medical Center; FP, fusion peptide; IC$_{50}$, median inhibitory concentration; SARS, severe acute respiratory syndrome; SP, signal peptide; TM, transmembrane domain.

mutant; results are shown in Figure 3A. HR1P alone was not detected in the gel (Figure 3A, *lanes 1–3*) because this peptide carries a net positive charge and thus migrated out of the gel under native electrophoresis condition [16]. HR2P-M2 alone migrated rapidly (*lane 4*), whereas the mixture of HR2P-M2 and HR1P or its mutant migrated more slowly in the gel (*lanes 5–7*). Similarly, HR2P-F alone exhibited a rapidly migrating band (*lane 8*),

whereas the mixture of HR2P-M2 and HR1P or its mutants migrated more slowly in the gel (*lanes 9–11*). These results confirmed that both HR2P-M2 and HR2P-F interact with HR1P and its mutants to form 6-HB.

We subsequently assessed the ability of HR2P-M2 to inhibit 6-HB formation between MERS-CoV HR1 and HR2 peptides using FN-PAGE, as described elsewhere [16, 19, 22]. As shown
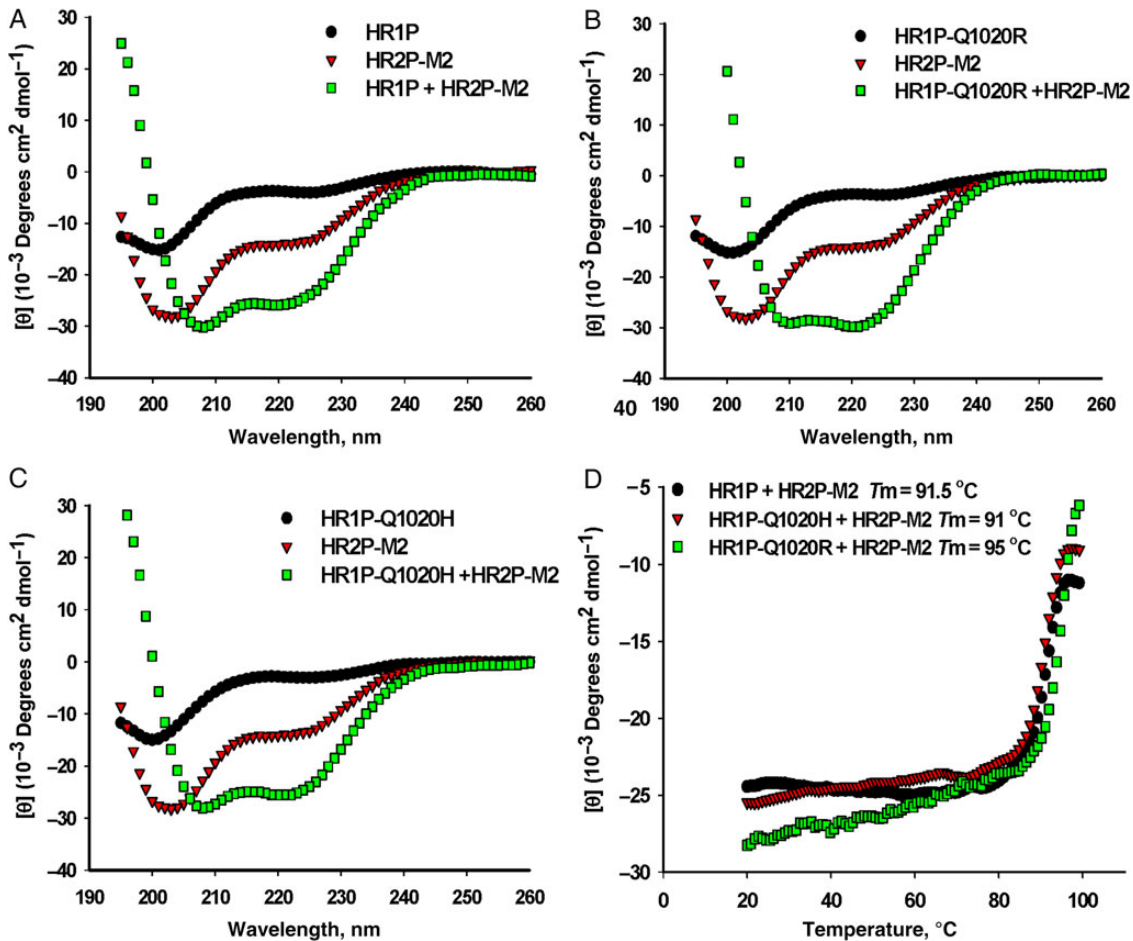
Figure 2. Interaction of HR2P-M2 with HR1P or its mutant to form stable α-helical complexes. Circular dichroism spectroscopic analysis shows the secondary structure of the complexes formed by HR2P-M2 peptide and HR1P (*A*), HR1P-Q1020H (*B*), or HR1P-Q1020R (*C*). The circular dichroism spectra are shown for the individual peptides and complexes in phosphate buffer (pH 7.2) at 4°C. *D*, Circular dichroism signal at 222 nm for the HR1P/HR2P complex as a function of temperature. The curve of the first derivative ($d[\theta]/dT$) against temperature (*T*) was used to determine the *T*m value. Abbreviation: *T*m, thermal unfolding transition.

---

in Figure 3*B*, the sample containing only HR2P-F (lane 2) displayed a single fluorescence band located in the lower portion of the gel, whereas the mixture of HR1P and HR2P-F (lane 3) migrated more slowly. This band corresponded to 6-HB. When increasing concentrations of HR2P-M2 were incubated with HR1P at 37°C for 30 minutes before addition of HR2P-F (lanes 4–6), the fluorescence intensity of the HR2P-F band gradually increased, whereas that of bands of the complexes corresponding to 6-HB decreased, suggesting that HR2P-M2 inhibited 6-HB formation between the HR1P and HR2P-F in a dose-dependent manner.

Inhibition of MERS-CoV Infection in Ad5-hDPP4–Transduced Mice by Intranasal Administration of HR2P-M2

Because mice are impervious to infection with MERS-CoV [31], we sensitized them to infection by transduction with Ad5-hDPP4 [27] before testing the in vivo efficacy of HR2P-M2

against infection by MERS-CoV EMC/2012, or recombinant MERS-CoV carrying Q1020R or Q1020H mutations in the S protein. HR2P-M2 (200 μg) or PBS (control) was intranasally administered to Ad5-hDPP4–transduced mice 6 hours before challenge with 1×10^5 PFUs of MERS-CoV in a total DMEM volume of 50 μL. As shown in Figure 4, viral titers in the lungs of PBS-treated mice challenged with recombinant MERS-CoV carrying WT, Q1020R, or Q1020H S protein peaked at about 10^6, 10^5, and 10^5 PFUs/g, respectively. Strikingly, titers in the lungs of mice treated with HR2P-M2 and challenged with WT, Q1020R, and Q1020H MERS-CoV were decreased to 10^3 PFUs/g (WT) or below the limit of detection (Q1020R and Q1020H), representing >1000-fold reduction of viral titers in lung. The limit of detection of the viral titers in our assay was 10^2 PFUs/g, suggesting that mice intranasally treated with HR2P-M2 6 hours before challenge with MERS-CoV or its variants were highly protected from MERS-CoV infection.
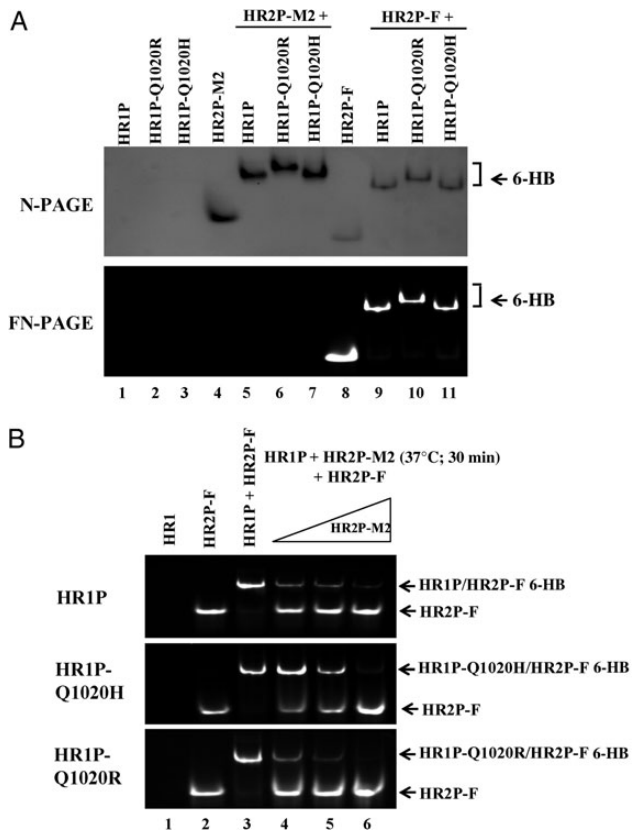
Figure 3. Inhibition of HR2P-M2 on 6-HB formation between HR1 and HR2 peptides. *A,* Determination of 6-HB formation between HR2P-M2, or HR2P-F, and HR1P, or its mutant, with native polyacrylamide gel electrophoresis (N-PAGE) (*upper panel*) and fluorescence N-PAGE (FN-PAGE) (*lower panel*). Mixtures of HR1 and HR2 peptides at a final concentration of 40 μmol/L were incubated at 25°C for 30 minutes before electrophoresis. Fluorescence bands in the gel were first imaged using a FluorChem 8800 Imaging System and a transillumination UV light source. The gel was then stained with Coomassie blue and imaged again with the FluorChem 8800 Imaging System. *B,* HR1P was incubated with HR2P-M2, followed by the addition of HR2P-F, and inhibitory activity against 6-HB formation was detected with FN-PAGE. Specifically, HR1P was incubated with increasing concentrations (40, 60, and 80 μmol/L) of HR2P-M2 at 37°C for 30 minutes before addition of HR2P-F. After incubation at 37°C for another 30 minutes, the mixture was loaded to the gel. Fluorescence bands in the gel were first imaged with the FluorChem 8800 Imaging System using a transillumination UV light source. Abbreviations: 6-HB, six-helix bundle; HR, heptad repeat.

Intranasal Application of HR2P-M2 and IFN-β in Combination, Before or After Viral Challenge, for Protection of Ad5-hDPP4–Transduced Mice From MERS-CoV Infection

Studies using the HIV-specific peptide enfuvirtide demonstrated the emergence of resistance in the HR1 domain of HIV during prolonged exposure [32]. Therefore, to diminish the likelihood of this occurrence and to provide an additional layer of protection in the event of any emerging resistant virus, we included IFN-β in our prophylactic and therapeutic regimens. IFN-β potently inhibited MERS-CoV infection in cell culture
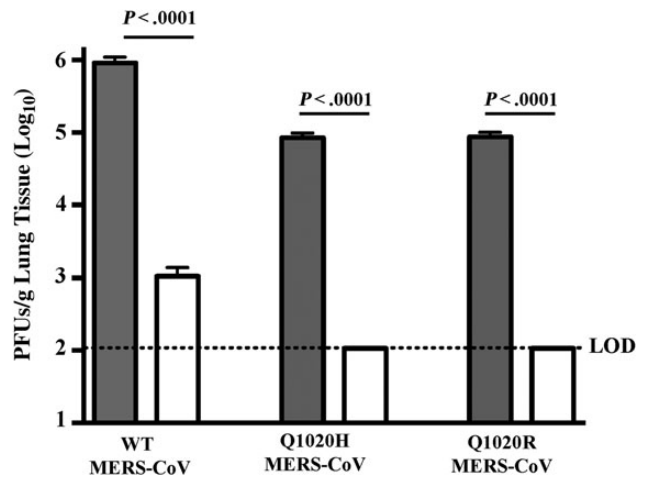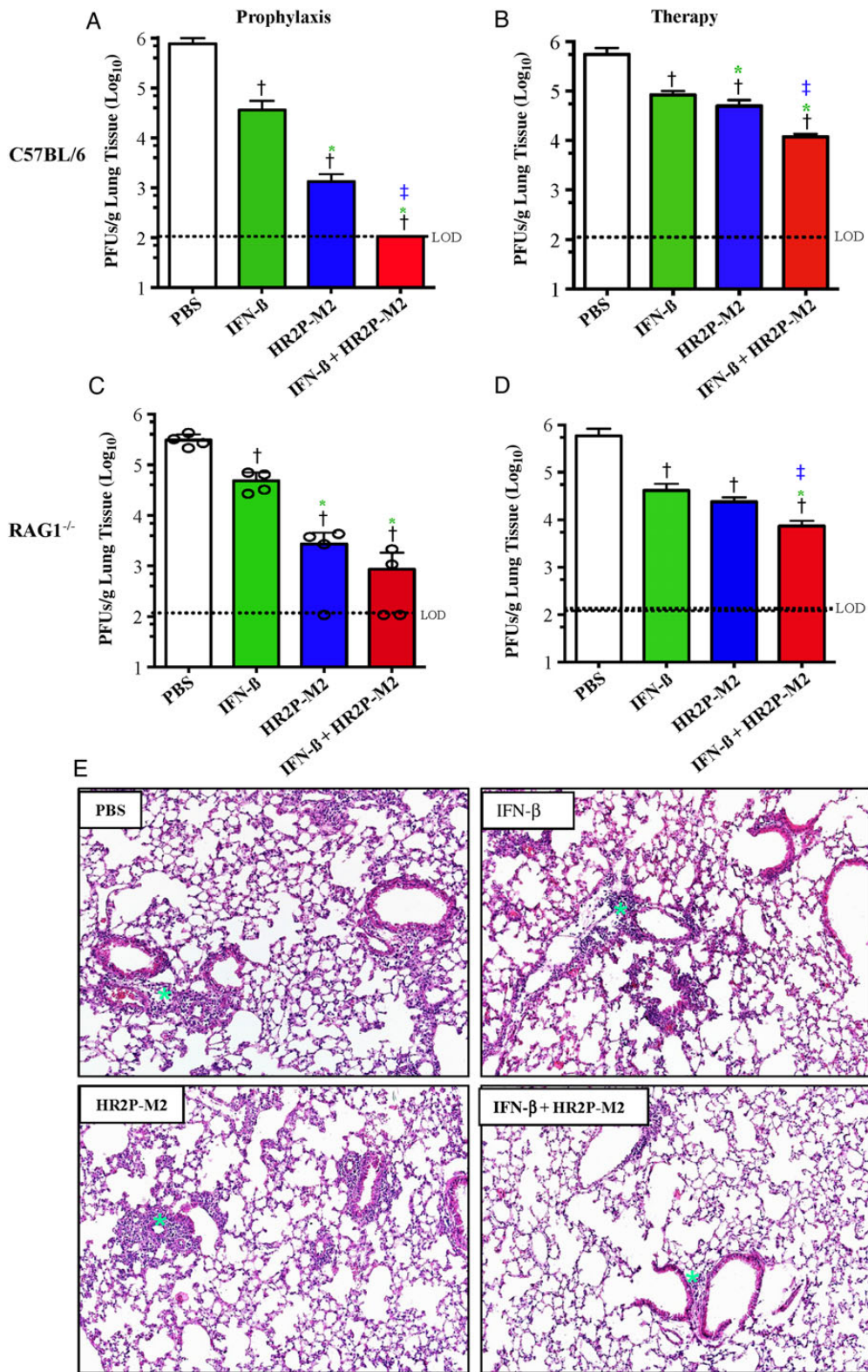

Figure 4. Inhibition of Middle East respiratory syndrome coronavirus (MERS-CoV) infection in Ad5–human dipeptidyl peptidase 4 (hDPP4)–transduced mice by intranasal administration of HR2P-M2 alone before viral challenge. Ad5-hDPP4–transduced C57BL/6 mice were treated intranasally with 200 μg of HR2P-M2 or phosphate-buffered saline (PBS) only, respectively, as described in "Materials and Methods" section. Six hours later, mice were infected with 1×10^5 plaque-forming units (PFUs) of wild-type (WT) MERS-CoV, Q1020H-MERS-CoV or Q1020R-MERS-CoV in 50 μL of Dulbecco's modified Eagle medium. Viral titers were determined on day 3 after infection, as described elsewhere [27]. Data are representative of 2 independent experiments with 3–4 mice per group per experiment. Statistical significance was determined with unpaired Student *t* test (comparing PBS-treated and HR2P-M2–treated groups in WT MERS-CoV, Q1020H-MERS-CoV or Q1020R-MERS-CoV–infected C56BL/6 mice). Abbreviations: Ad5, adenovirus serotype 5; HR, heptad repeat.

[33], and Zhao et al [27] showed previously that IFN-β treatment, before or after MERS-CoV challenge, significantly accelerated the kinetics of virus clearance.

Initially, we tested the in vivo efficacy of IFN-β, HR2P-M2, and their combination as prophylaxis in MERS-CoV–infected C57BL/6 mice. Mice were transduced with Ad5-hDPP4 and treated 5 days later with intranasal administration of PBS, IFN-β, HR2P-M2, or IFN-β/HR2P-M2. Six hours later, mice were challenged with MERS-CoV, and viral titers were measured 72 hours after infection. Titers were significantly reduced in all treated groups, with complete clearance observed in mice treated with IFN-β/HR2P-M2 (Figure 5*A*). To assess whether these drugs could be used therapeutically, MERS-CoV–infected Ad5-hDPP4–transduced mice were treated 12 and 36 hours after infection, with PBS, IFN-β, HR2P-M2, or IFN-β/HR2P-M2, and viral titers were measured 96 hours after infection.

As shown in Figure 5*B*, titers were significantly decreased in all inhibitor-treated groups ($P < .003$ for comparison with PBS-treated group), with the greatest reduction observed in IFN-β/HR2P-M2–treated mice. Moreover, treatment with HR2P-M2 alone resulted in significant reduction in the viral titers in comparison to IFN-β alone treatment groups (Figure 5*A* and *B*). Additional cohorts of control mice and mice treated

Figure 5. Inhibition of Middle East respiratory syndrome coronavirus (MERS-CoV) infection in Ad5–human dipeptidyl peptidase 4 (hDPP4)–transduced mice by intranasal application of HR2P-M2-containing regimens before and/or after viral challenge. *A-D*, Determination of viral titers in the lungs of MERS-CoV–infected Ad5-hDPP4–transduced C57BL/6 and RAG1$^{-/-}$ mice treated with interferon (IFN) β, HR2P-M2, or both. *A, C,* Ad5-hDPP4–transduced C57BL/6 (*A*) and RAG1$^{-/-}$ mice (*C*) were intranasally treated with 2000 U of IFN-β, 200 μg of HR2P-M2, both IFN-β (2000 U) and HR2P-M2 (200 μg), or phosphate-buffered saline (PBS) only, as described in "Materials and Methods" section. Six hours later, mice were infected with 1 × 10⁵ plaque-forming units (PFUs) of MERS-CoV in a total volume of 50 μL of Dulbecco's modified Eagle medium (DMEM). Viral titers were determined on day 3 after infection, as described elsewhere [27]. *B, D,* Ad5-hDPP4–transduced C57BL/6 (*B*) and RAG1$^{-/-}$ mice (*D*) were infected intranasally with 1 × 10⁵ PFUs of MERS-CoV in a total

therapeutically were killed 7 days after infection, and their lungs were examined for histological changes. In agreement with a previous report [27], the lungs of MERS-CoV–infected mice showed perivascular, peribronchial, and interstitial infiltrates, as well as alveolar septa thickening. However, infiltration was moderately reduced in mice treated with IFN-β and HR2P-M2 alone, with pathological changes most attenuated in the IFN-β/HR2P-M2–treated group, consistent with the effects on viral titers (Figure 5B and 5E). In no instance was a significant eosinophilic infiltrate detected.

Mice lacking T and B cells (RAG1$^{-/-}$, recombination activation gene 1$^{-/-}$) were unable to clear MERS-CoV with virus detected in the lungs for ≥30 days (data not shown). Therefore, to determine whether IFN-β, HR2P-M2, or IFN-β/HR2P-M2 could enhance virus clearance in the absence of adaptive immune response, MERS-CoV–infected Ad5-hDPP4–transduced RAG1$^{-/-}$ mice were treated prophylactically or therapeutically, as described above for C57BL/6 mice. Prophylactic treatment resulted in enhanced virus clearance at 72 hours after infection, with complete virus clearance in 1/8 HR2P-M2 and 4/8 IFN-β/HR2P-M2 mice (Figure 5C). Similarly, measurement of viral titers at 96 hours after infection, following therapeutic treatment at 12 and 36 hours, revealed significant decreases in titers after all treatments ($P < .005$ vs PBS treatment). As before, viral titers were most reduced in mice treated with IFN-β/HR2P-M2 (Figure 5B and 5D).

DISCUSSION

Previous studies have demonstrated that peptides derived from MERS-CoV S protein HR2 potently inhibit virus entry, but our present study is the first to show that the peptide functions in the infected lung. From these results, we conclude that peptide is stable in the milieu of the MERS-CoV–infected lung and that intranasal administration delivers peptide to areas of infection sufficient quantities to inhibit virus entry.

So far, no specific antiviral drug has been developed to prevent or treat MERS-CoV infection. Falzarano et al [34] demonstrated that the combination of ribavirin and IFN-α2b administered to rhesus macaques within 8 hours of inoculation with MERS-CoV resulted in beneficial effects in reducing virus replication,

lung injury, and inflammation, thus improving clinical outcome. This combination was also provided to several severely ill patients, and though it reduced the mortality rate 14 days after treatment, it did not show beneficial effects by 28 days, possibly because of late administration [35]. Ribavirin/IFN-a2b in combination with HR2P-M2 may diminish morbidity and mortality rates more successfully than either therapy alone. Recently, several compounds from Food and Drug Administration–approved drug libraries were reported to have inhibitory activity against MERS-CoV replication in cell culture [36, 37]. Liu et al demonstrated that some of these MERS-CoV replication inhibitors could inhibit clathrin-mediated endocytosis, but most of them did not inhibit MERS-CoV S protein–mediated membrane fusion, and none was able to inhibit 6-HB formation [38]. Therefore, these small-molecule MERS-CoV replication inhibitors seem to have mechanisms of action different from that of the peptide MERS-CoV fusion inhibitor HR2P [16].

The HR1 domain in MERS-CoV S protein is the most important target for development of MERS-CoV fusion inhibitors because this region is relatively conserved. Only a single change in the amino acid at position 1020 in the HR1 domain, namely, Q1020H or Q1020R mutations, has been reported [29, 30]. In the present study, we showed that the viruses expressing Q1020H or Q1020R actually grow less well in mouse lung, although they are still potently inhibited by HR2P-M2. Therefore, the peptide targeting the HR1 domain is expected to be effective against most MERS-CoV strains identified thus far.

IFN-β potently inhibited MERS-CoV infection in an in vitro cell culture [34, 39] and significantly accelerated virus clearance when delivered before or after MERS-CoV challenge [27]. In the present study, we demonstrated that in mice intranasally treated with HR2P-M2 or IFN-β alone or in combination 6 hours before viral challenge, viral titers in lung were significantly reduced in all treated groups, with complete clearance observed in mice treated with the IFN-β/HR2P-M2 combination (Figure 5A), verifying their in vivo efficacy for prophylactic treatment. We chose to deliver HR2P-M2 and IFN-β intranasally because MERS is predominantly a respiratory tract infection. Because no autopsy or surgical specimens are available from patients with MERS, it is not known whether a clinically relevant infection occurs in other organs. Furthermore, MERS-CoV is

---

Figure 5 continued. volume of 50 μL of DMEM. At 12 hours and 36 hours after infection, mice were treated intranasally with 2000 U of IFN-β, 200 μg of HR2P-M2, both IFN-β (2000 U) and HR2P-M2 (200 μg), or PBS only. Viral titers were determined on day 4 after infection. Data are representative of 2 independent experiments with 4 mice per group per experiment. Statistical significance was determined using unpaired Student t test. *A*, †*P* < .001 (PBS vs other groups); **P* < .02 (IFN-β vs other treated groups); ‡*P* < .01 (HR2P-M2 vs IFN-β + HR2P-M2). *B*, †*P* < .01 (PBS vs other groups); **P* < .03 (IFN-β vs other treated groups); ‡*P* < .01 (HR2P-M2 vs IFN-β + HR2P-M2). *C*, †*P* < .002 (PBS vs other groups); **P* < .01 (IFN-β vs other treated groups). *D*, †*P* < .01 (PBS vs other groups); *,‡*P* < .01, IFN-β + HR2P-M2 vs IFN-β; ‡*P* < .01, IFN-β + HR2P-M2 vs HR2P-M2. *E*, Histological examination of lungs from MERS-CoV–infected, Ad5-hDPP4–transduced C57BL/6 mice at 7 days after infection. Ad5-hDPP4–transduced C57BL/6 mice were infected intranasally with 1 × 10^5 PFUs MERS-CoV in a total volume of 50 μL of DMEM. At 12 and 36 hours after MERS-CoV infection, mice were treated intranasally with 100 μL of PBS (50 + 50 μL at 10-minute intervals) containing 2000 U of IFN-β, 200 μg of HR2P-M2, both IFN-β (2000 U) and HR2P-M2 (200 μg), or PBS only, respectively. After mice were killed on day 7 after infection, lungs were removed, fixed in zinc formalin, and paraffin embedded; sections were stained with hematoxylin-eosin (original magnification, ×10). The green stars (asterisks) indicate the sites of infiltration. Abbreviations: Ad5, adenovirus serotype 5; HR, heptad repeat.

released from the apical side of respiratory tract cells [40]. Therefore, peptide delivered intranasally would be maximal at the site of infection.

Similarly, intranasal administration of the HR2P-M2/IFN-β combination also significantly reduced viral titers in the lungs of RAG1$^{-/-}$ mice, with complete virus clearance in 50% of the treated mice (Figure 5C), whereas untreated RAG1$^{-/-}$ mice were unable to clear MERS-CoV for ≥30 days, owing to a lack of T and B cells [27]. In addition, intranasal administration of HR2P-M2, IFN-β, and their combination to Ad5-hDPP4–transduced C57BL/6 and RAG1$^{-/-}$ mice at 12 and 36 hours after infection significantly reduced viral titers in all inhibitor-treated groups, compared with the PBS-treated mice, with titers reduced most in mice treated with the IFN-β/HR2P-M2 combination (Figure 5B and 5D). Pathological changes in the lungs, such as perivascular, peribronchial and interstitial infiltration, as well as alveolar septa thickening, were moderately reduced in groups treated with IFN-β or HR2P-M2 alone, with significant attenuation in the IFN-β/HR2P-M2–treated group (Figure 5E).

Unfortunately, no lung samples are available from MERS-CoV–infected patients; therefore, it is not known whether similar findings would be present in infected humans. However, based on studies of autopsy specimens from patients infected with SARS-CoV, it is likely that severely ill patients would exhibit diffuse alveolar damage. Other than marmosets, no animals experimentally infected with MERS-CoV develop similar disease severity, to our knowledge. Once a widely available animal model of severe disease is developed, it will be important to test IFN-β/HR2P-M2 for prophylactic and therapeutic efficacy. It may also be necessary to evaluate different routes of administration of IFN-β and HR2P-M2 if patients or experimentally infected animals are shown to develop significant systemic disease.

In conclusion, HR2P-M2, a peptide MERS-CoV fusion inhibitor specifically targeting the S protein HR1 domain, is highly effective in inhibiting in vitro and in vivo infection of divergent MERS-CoV strains. Intranasal application of HR2P-M2, especially in combination with IFN-β, showed high efficacy in accelerating MERS-CoV clearance in animals, suggesting good potential for further development as a prophylactic agent to protect high-risk populations, including healthcare workers and family members of patients infected with MERS-CoV. It also showed efficacy in the treatment of MERS-CoV–infected mice, indicating potential use as a therapeutic agent to treat MERS-CoV–infected patients.

Notes

References

1. Zaki AM, van Boheemen S, Bestebroer TM, Osterhaus ADME, Fouchier RAM. Isolation of a novel coronavirus from a man with pneumonia in Saudi Arabia. N Engl J Med 2012; 367:1814–20.
2. Assiri A, McGeer A, Perl TM, et al. Hospital outbreak of Middle East respiratory syndrome coronavirus. N Engl J Med 2013; 369:407–16.
3. Lu L, Liu Q, Du L, Jiang S. Middle East respiratory syndrome coronavirus (MERS-CoV): challenges in identifying its source and controlling its spread. Microbes Infect 2013; 15:625–9.
4. Memish ZA, Zumla AI, Assiri A. Middle East respiratory syndrome coronavirus infections in health care workers. N Engl J Med 2013; 368:2487–94.
5. Adney DR, van DN, Brown VR, et al. Replication and shedding of MERS-CoV in upper respiratory tract of inoculated dromedary camels. Emerg Infect Dis 2014; 20:1999–2005.
6. Gossner C, Danielson N, Gervelmeyer A, et al. Human-dromedary camel interactions and the risk of acquiring zoonotic Middle East respiratory syndrome coronavirus infection. Zoonoses Public Health 2014; doi:10.1111/zph.12171.
7. Memish ZA, Mishra N, Olival KJ, et al. Middle East respiratory syndrome coronavirus in bats, Saudi Arabia. Emerg Infect Dis 2013; 19:1819–23.
8. Reuss A, Litterst A, Drosten C, et al. Contact investigation for imported case of Middle East respiratory syndrome, Germany. Emerg Infect Dis 2014; 20:620–5.
9. Perlman S, McCray PB Jr. Person-to-person spread of the MERS coronavirus—an evolving picture. N Engl J Med 2013; 369:466–7.
10. Chen Y, Rajashankar KR, Yang Y, et al. Crystal structure of the receptor-binding domain from newly emerged Middle East respiratory syndrome coronavirus. J Virol 2013; 87:10777–83.
11. Du L, Zhao G, Kou Z, et al. Identification of a receptor-binding domain in the S protein of the novel human coronavirus Middle East respiratory syndrome coronavirus as an essential target for vaccine development. J Virol 2013; 87:9939–42.
12. Lu G, Hu Y, Wang Q, et al. Molecular basis of binding between novel human coronavirus MERS-CoV and its receptor CD26. Nature 2013; 500:227–31.
13. Mou H, Raj VS, van Kuppeveld FJ, Rottier PJ, Haagmans BL, Bosch BJ. The receptor binding domain of the new MERS coronavirus maps to a 231-residue region in the spike protein that efficiently elicits neutralizing antibodies. J Virol 2013; 87:9379–83.
14. Wang N, Shi X, Jiang L, et al. Structure of MERS-CoV spike receptor-binding domain complexed with human receptor DPP4. Cell Res 2013; 23:986–93.
15. Raj VS, Mou H, Smits SL, et al. Dipeptidyl peptidase 4 is a functional receptor for the emerging human coronavirus-EMC. Nature 2013; 495:251–4.
16. Lu L, Liu Q, Zhu Y, et al. Structure-based discovery of Middle East respiratory syndrome coronavirus fusion inhibitor. Nat Commun 2014; 5:3067.
17. Chan DC, Fass D, Berger JM, Kim PS. Core structure of gp41 from the HIV envelope glycoprotein. Cell 1997; 89:263–73.
18. Jiang S, Lin K, Strick N, Neurath AR. HIV-1 inhibition by a peptide. Nature 1993; 365:113.
19. Liu S, Xiao G, Chen Y, et al. Interaction between heptad repeat 1 and 2 regions in spike protein of SARS-associated coronavirus: implications for virus fusogenic mechanism and identification of fusion inhibitors. Lancet 2004; 363:938–47.
20. Wild CT, Shugars DC, Greenwell TK, McDanal CB, Matthews TJ. Peptides corresponding to a predictive alpha-helical domain of human

immunodeficiency virus type 1 gp41 are potent inhibitors of virus infection. Proc Natl Acad Sci USA **1994**; 91:9770–4.

21. Chen YH, Yang JT, Chau KH. Determination of the helix and beta form of proteins in aqueous solution by circular dichroism. Biochemistry **1974**; 13:3350–9.

22. Liu S, Zhao Q, Jiang S. Determination of the HIV-1 gp41 postfusion conformation modeled by synthetic peptides: applicable for identification of the HIV-1 fusion inhibitors. Peptide **2003**; 24:1303–13.

23. Lu M, Blacklow SC, Kim PS. A trimeric structural domain of the HIV-1 transmembrane glycoprotein. Nat Struct Biol **1995**; 2:1075–82.

24. Chou TC. Theoretical basis, experimental design, and computerized simulation of synergism and antagonism in drug combination studies. Pharmacol Rev **2006**; 58:621–81.

25. He Y, Lu H, Siddiqui P, Zhou Y, Jiang S. Receptor-binding domain of severe acute respiratory syndrome coronavirus spike protein contains multiple conformation-dependent epitopes that induce highly potent neutralizing antibodies. J Immunol **2005**; 174:4908–15.

26. Zhao G, Du L, Ma C, et al. A safe and convenient pseudovirus-based inhibition assay to detect neutralizing antibodies and screen for viral entry inhibitors against the novel human coronavirus MERS-CoV. Virol J **2013**; 10:266.

27. Zhao J, Li K, Wohlford-Lenane C, et al. Rapid generation of a mouse model for Middle East respiratory syndrome. Proc Natl Acad Sci U S A **2014**; 111:4970–5.

28. Fehr AR, Perlman S. Coronaviruses: an overview of their replication and pathogenesis. Methods Mol Biol **2015**; 1282:1–23.

29. MERS-coronavirus sequence acknowledgements. **2014**. http://epidemic. bio.ed.ac.uk/MERS_sequences. Accessed 23 May 2015.

30. Cotten M, Watson SJ, Zumla AI, et al. Spread, circulation, and evolution of the Middle East respiratory syndrome coronavirus. MBio **2014**; 5: e01062-13.

31. Cockrell AS, Peck KM, Yount BL, et al. Mouse dipeptidyl peptidase 4 is not a functional receptor for Middle East respiratory syndrome coronavirus infection. J Virol **2014**; 88:5195–9.

32. Xu L, Pozniak A, Wildfire A, et al. Emergence and evolution of enfuvirtide resistance following long-term therapy involves heptad repeat 2 mutations within gp41. Antimicrob Agents Chemother **2005**; 49:1113–9.

33. Hart BJ, Dyall J, Postnikova E, et al. Interferon-beta and mycophenolic acid are potent inhibitors of Middle East respiratory syndrome coronavirus in cell-based assays. J Gen Virol **2014**; 95:571–7.

34. Falzarano D, de Wit E, Rasmussen AL, et al. Treatment with interferon-[alpha]2b and ribavirin improves outcome in MERS-CoV-infected rhesus macaques. Nat Med **2013**; 19:1313–7.

35. Al-Tawfiq JA, Momattin H, Dib J, Memish ZA. Ribavirin and interferon therapy in patients infected with the Middle East respiratory syndrome coronavirus: an observational study. Int J Infect Dis **2014**; 20:42–6.

36. de Wilde AH, Jochmans D, Posthuma CC, et al. Screening of an FDA-approved compound library identifies four small-molecule inhibitors of Middle East respiratory syndrome coronavirus replication in cell culture. Antimicrob Agents Chemother **2014**; 58:4875–84.

37. Dyall J, Coleman CM, Hart BJ, et al. Repurposing of clinically developed drugs for treatment of Middle East respiratory coronavirus infection. Antimicrob Agents Chemother **2014**; 58:4885–93.

38. Liu Q, Xia S, Sun Z, et al. Testing of Middle East respiratory syndrome coronavirus replication inhibitors for the ability to block viral entry. Antimicrob Agents Chemother **2015**; 59:742–4.

39. Chan JF, Chan KH, Kao RY, et al. Broad-spectrum antivirals for the emerging Middle East respiratory syndrome coronavirus. J Infect **2013**; 67:606–16.

40. Zielecki F, Weber M, Eickmann M, et al. Human cell tropism and innate immune system interactions of human respiratory coronavirus EMC compared to SARS-coronavirus. J Virol **2013**; 87:5300–4.